Clin Exp Dermatol 2024; **49**:356–363
https://doi.org/10.1093/ced/llad405
Advance access publication date: 23 November 2023

CED
Clinical and Experimental Dermatology
Original Article

Combined WNT-activated deep-penetrating/plexiform melanocytoma: insights into clinicopathological and molecular characterization

Paola Castillo[1,2,3] **Natalia Castrejon**[1,2] **Marta Marginet**[1] **Daniela Massi**[4,5] **Francesc Alamon**[6] **Cristina Teixido**[1,2,3] **Carla Montironi**[1] **Adriana Garcia-Herrera**[1,2,3] **Raquel Albero-Gonzalez**[1] **Jessica Matas**[7] **Susana Puig**[2,3,5,6] **and Llucia Alos**[1,2,3,5]

Departments of [1]Pathology; [6]Dermatology and [7]Opthamology, Hospital Clinic of Barcelona, Barcelona, Spain
[2]University of Barcelona. Barcelona, Spain
[3]August Pi i Sunyer Biomedical Research Institute (IDIBAPS), Barcelona, Spain
[4]Section of Anatomical Pathology, Department of Health Sciences, University of Florence. Florence, Italy
[5]European Organisation for Research and Treatment of Cancer (EORTC), Melanoma Group

Correspondence: Llucia Alos. Email: lalos@clinic.cat

Abstract

Background A combined deep-penetrating tumour redefined as WNT-activated deep-penetrating/plexiform melanocytoma (DPM), may pose challenging clinical and histological diagnoses.

Objectives To review the clinicopathological characteristics of combined DPMs and characterize the molecular profile of atypical and malignant forms.

Methods The study included 51 patients with combined DPMs diagnosed at the Hospital Clinic of Barcelona and the University of Florence between 2012 and 2020. Clinical data, dermoscopy images (when available) and histological characteristics were reviewed. Immunohistochemistry for β-catenin, LEF1, HMB45, Ki67, p16 and PRAME (preferentially expressed antigen in melanoma) was performed. Atypical forms underwent next-generation sequencing (NGS) panel analysis, including driver genes implicated in DPMs, *TERT*-promoter (p) mutations and the investigation of the 9p21 locus via fluorescence *in situ* hybridization.

Results Among the 51 patients (32 females and 19 males, age range 4–74 years), 68% with available clinical data (15/22) were initially suspected of having melanoma. Except for one patient, complete excision resulted in no recurrences or metastases. One patient who had an incompletely excised combined DPM developed a lymph node melanoma metastasis 10 years later. In the 51 patients, 10 samples (20%) showed atypical histological features; 7 (14%) exhibited a significant loss of p16 expression; and 2 (4%) showed a high-proliferative index (Ki67 over 5%). NGS analysis in 11 patients revealed a double mutation *BRAF*^{V600E} and exon 3 *CTNNB1*; no *TERT*p mutations were detected.

Conclusions Clinical suspicion of melanoma is common in combined DPMs, but malignant progression is infrequent in tumours lacking high-grade atypia or proliferation. These findings are congruent with the consideration of these lesions as intermediate-grade tumours or melanocytomas.

What is already known about this topic?

- Deep-penetrating tumours have been renamed as WNT-activated deep-penetrating/plexiform melanocytomas (DPMs).
- Combined DPMs may exhibit clinical and histopathological features that can pose diagnostic challenges.

What does this study add?

- This study presents a series of 51 combined DPMs, with analysis of clinical and histopathological features, as well as the molecular profile of the atypical forms.
- The study adds data supporting the complete excision of combined DPMs because of their potential, albeit low, for malignant transformation.

Accepted: 14 November 2023

Combined naevi are tumours composed of two different melanocytic cell types, often involving a common acquired or congenital-type naevus combined with a second component, such as blue naevus, deep-penetrating tumour, Spitz tumour and other less frequent melanocytic tumour types.[1,2]

The current World Health Organization classification of skin tumours emphasizes the integration of morphology and molecular content in the categorization of melanocytic tumours and accepts the term melanocytoma as an intermediate step from a naevus to a melanoma.[3] Combined WNT-activated deep-penetrating/plexiform melanocytoma (DPM) develops from a pre-existing common acquired or congenital naevus harbouring MAPK activation (e.g. *BRAF*- or *NRAS*-mutated naevus) in which a clone acquires additional molecular alterations that activate the WNT pathway (through β-catenin or *APC* mutations)[3–5] and encompasses distinctive histological features.[3]

Combined DPMs may present with a large diversity of clinical and histological patterns, and now include the previously termed combined plexiform naevus,[6] clonal naevus,[7] naevus with phenotypic heterogeneity[8] and inverted type-A naevus.[9] DPMs encompass deep-penetrating naevus (DPN) or low-grade melanocytomas, as well as DPN with atypical features or high-grade melanocytomas.[3] Histological features in the DPM component, such as dermal mitoses, mild-to-moderate proliferative index assessed by Ki67, moderate cytologic atypia (e.g. nuclear pleomorphism) and lack of in-depth maturation can be seen even in low-grade tumours[10,11] and can cause diagnostic difficulties.[1]

The potential of regional lymph node metastases presentation and further progression to a malignant deep-penetrating tumour, showing the clinical and histopathology of an aggressive melanoma, have been previously documented.[12–15] These studies have revealed the molecular alterations that characterize this progression, including more than three DNA copy-number (CN) alterations, *TERT*-promoter (p) mutations and a characteristic immunohistochemical profile: loss of p16 expression, a Ki67 proliferative index over 5% and positivity for PRAME (preferentially expressed antigen in melanoma).[13,14]

Since this recent classification, there have been no reports of series including a large number of these melanocytomas, to the best of our knowledge. This study aimed to review a series of combined DPMs, with a special interest in atypical forms and inclusion of clinicopathological features and follow-up of patients, in order to deepen knowledge about these recently reclassified melanocytic lesions.

Materials and methods

Patients and samples

The files of the Pathology Department of the Hospital Clinic, University of Barcelona, and of the Department of Health Sciences at the University of Florence were reviewed, searching for cases of patients diagnosed with combined DPM from 2012 to 2020. Haematoxylin and eosin-stained slides were examined, and architectural and cytological characteristics were recorded. Atypical features were considered for tumours with size $\geq$ 5 mm, poor circumscription, asymmetry, expansile growth, high-grade atypia, mitoses $>$ 2 per mm^2, atypical mitoses and necrosis.[3] High-grade atypia was considered when tumoral cells showed enlarged nuclei ($\geq$ 1.5 times the size of resting basal keratinocytes), pleomorphism, hyperchromasia and presence of nucleoli. Moderate atypia was considered when only scattered cells showed some of these nuclear characteristics.

Patient data were anonymized and clinical data at diagnosis and patient outcomes were obtained from electronic medical records. Clinical and dermoscopy pictures were also reviewed when available. This study adhered to the principles of the Declaration of Helsinki, and patients provided their written informed consent to participate.

Immunohistochemical study

The immunohistochemical studies were performed on formalin-fixed, paraffin-embedded tissue sections and on an automated immunostainer, according to the manufacturer's protocol (Ventana BenchMark ULTRA platform; Ventana, Tucson, AZ, USA). The following monoclonal antibodies were used: β-catenin (clone 14; Ventana), LEF1 (clone EPR2029Y; Abcam, Cambridge, UK), anti-Melanosome (clone HMB45; Ventana), Ki67 (clone 44469; Ventana), p16 (clone E6H4; Ventana); double stain Melan-A + Ki67 (clones A103 and 44469; both Ventana), PRAME (preferentially expressed antigen in melanoma, clone QR005; Quimigen, Madrid, Spain).

Immunohistochemical results were evaluated by two pathologists (P.C. and L.A.).

9p21 analysis by fluorescence *in situ* hybridization

Fluorescence *in situ* hybridization (FISH) analysis for 9p21 was performed using the Vysis LSI *CDKN2A* SpectrumOrange/CEP 9 SpectrumGreen probe kit (Abbott Molecular Inc., Des Plaines, IL, USA) in all those with atypical features and in tumours showing p16 loss (tumours completely negative or showing dermal tumoral nests completely negative for p16). FISH signals were enumerated in at least 100 nonoverlapping intact nuclei. FISH homozygous deletion of *CDKN2A* was considered when no 9p21 locus signal was detected in more than 30% of the total assessed tumour cells; FISH heterozygous deletion of *CDKN2A* was considered when only one 9p21 locus signal was detected in more than 30% of tumour cells.[16]

Next-generation sequencing and *TERT*-promoter mutation

Next-generation sequencing (NGS) and detection of *TERT*p mutations by Sanger sequencing were performed in combined DPMs showing atypical characteristics. Macrodissection of the DPM component, DNA and RNA extraction using appropriate kits (QIAGEN, Hilden, Germany) were performed before NGS. NGS was carried out using the Oncomine Focus Assay (ThermoFisher, Waltham, MA, USA), which includes amplicons covering hotspot regions of *AKT1*, *ALK*, *APC*, *AR*, *BRAF*, *CDK4*, *CTNNB1*, *DDR2*, *EGFR*, *ERBB2*, *ERBB3*, *ERBB4*, *ESR1*, *FGFR2*, *FGFR3*, *GNA11*, *GNAQ*, *HRAS*, *IDH1*, *IDH2*, *JAK1*, *JAK2*, *KIT*, *KRAS*, *MAP2K1*, *MAP2K2*, *MET*, *MTOR*, *NRAS*, *PDGFRA*, *PIK3CA*, *RAF1*, *RET*, *ROS1* and *SMO*; CN variations (*AKT1*, *ALK*, *AR*,

BRAF, *CCND1*, *CDK4*, *CDK6*, *EGFR*, *ERBB2*, *FGFR1*, *FGFR2*, *FGFR3*, *FGFR4*, *KIT*, *KRAS*, *MET*, *MYC*, *MYCN*, *PDGFRA* and *PIK3CA*); and fusions (*ABL1*, *AKT3*, *ALK*, *AXL*, *BRAF*, *EGFR*, *ERBB2*, *ERG*, *ETV1*, *ETV4*, *ETV5*, *FGFR1*, *FGFR2*, *FGFR3*, *MET*, *NTRK1*, *NTRK2*, *NTRK3*, *PDGFRA*, *PPARG*, *RAF1*, *RET* and *ROS1*).

Polymerase chain reaction amplification of the *TERT*p region and direct sequencing were performed following standard protocols.

Fluorescence *in situ* hybridization melanoma multiprobe and copy-number array

Multiprobe FISH for melanoma and CN array (Oncoscan; ThermoFisher) were performed in samples from the patient with the combined DPM that developed metastatic melanoma, from both the primary tumour sample and the melanoma sample. A commercially available four-colour FISH probe set (Abbott Molecular) targeting *RREB1* on 6p25; *MYB* on 6q23; and *CCND1* on 11q13 and the chromosome 6 centromeric region was applied as previously described.[17]

Gains and losses and CN neutral-loss of heterozygosity (CNN-LOH) regions from Oncoscan arrays were evaluated using Nexus Biodiscovery v9.0 software (Biodiscovery, Hawthorne, CA, USA). The human reference genome was GRCh37/hg19. CN alterations with a minimum size of 100 kb and CNN-LOH larger than 5 Mb were considered informative.

Statistical analyses

The results of quantitative variables are given as median values and range. Qualitative variables are given as absolute and relative frequencies (percentages). Data were analysed with the SPSS statistical package (version 23.0; IBM, Armonk, NY, USA).

Results

In total, 51 combined DPMs were selected, 41 from patients at the Hospital Clinic of Barcelona and 10 from the University of Florence.

Clinicopathological characteristics at diagnosis

The clinicopathological characteristics are summarized in Table 1, and representative pictures are shown in Figures 1–4.

Lesions appeared slightly more frequently in female patients (63%) and located on the trunk (41%). Of the 11 patients with locations on the head and neck, seven (64%) affected the eyelid conjunctiva (Figure 1).

Clinical characteristics

Changes in size and/or increased dark pigmentation were seen in 16 out of 22 patients (73%) with available clinical data. A clinical diagnosis of malignant melanoma was suspected in 15 of these 22 patients (68%). Dermoscopy features were collected in 8 of the 51 patients (16%). A growing structureless area showing blue and grey colours over a naevus component was the most frequent image, as seen in seven patients. Asymmetry was also observed in five patients (Figure 2). Signs of noticeable vascularization were also frequent, including erythema, comma vessels and polychromatism (Figure 3). No white lines, chaotic architecture (an asymmetrical combination of colours and patterns) or other melanoma clues were seen.

One patient with a previously incompletely excised combined DPM on the left leg with a deep margin presented with a melanoma metastasis in the ipsilateral inguinal lymph node 10 years later (Figure 4). For the rest of the 50 patients with available follow-up, no lesion recurred or metastasized during a period from 2 to 11 years (median 6.5 years), after complete surgical excision of the lesion.

Table 1 Clinicopathological and molecular characteristics of the combined WNT-activated deep-penetrating/plexiform melanocytomas (DPMs) of the 51 patients assessed

Characteristics	Results
Age, years; median (range)	33 (4–74)
Sex	
Female	32 (63)
Male	19 (37)
Location	
Trunk	21 (41)
Extremities	17 (33)
Head and neck	11 (22)
Not available	2 (4)
Size DPM component, mm; median (range)	
Diameter	3.5 (1.0–6.0)
Depth	1.2 (0.7–4.5)
Atypical histological features[a]	10 (20)
IHC p16 loss[b]	7 (14)
IHC Ki67 over 5%	2 (4)
IHC PRAME positivity	0
9p21 FISH[c]	
No anomalies	12 (92)
CDKN2A heterozygous loss	1 (8)
CDKN2A homozygous loss	0
NGS[c]	
BRAF^{V600E} + exon 3 *CTNNB1*	11 (85)
Not available	2 (15)
Follow-up	
Recurrences	0
Melanoma development	1 (2)

Data are *n* (%) unless otherwise indicated. IHC, immunohistochemistry; FISH, fluorescence *in situ* hybridization; NGS, next-generation sequencing; PRAME, preferentially expressed antigen in melanoma. [a]Atypical histological features included size ≥ 5 mm, expansile growth and high-grade atypia. [b]IHC p16 loss was considered when complete loss of groups of cells was seen. [c]9p21 FISH and NGS were performed in 13 patients with atypical histological features and/or aberrant IHC (p16 loss and Ki67 proliferative antigen > 5%).

Pathological and immunohistochemical results

Lesions were composed of two different types of melanocytic cells. The naevomelanocytic component was a common naevus (33 patients, 65%) or a naevus showing congenital-type features (18 patients, 35%). The DPM component displayed symmetrically in the centre of the combined naevus in 26 patients (51%) and asymmetrically in 25 patients (49%). The DPM component measured from 1.0 to 6.0 mm large (median 3.5 mm) and from 0.7 to 4.5 mm deep (median 1.2 mm). It was displayed in the middle and deep dermis in most patients, but in five (10%), two of them in the conjunctiva, the DPM component was mainly superficial and displayed above the common naevus.

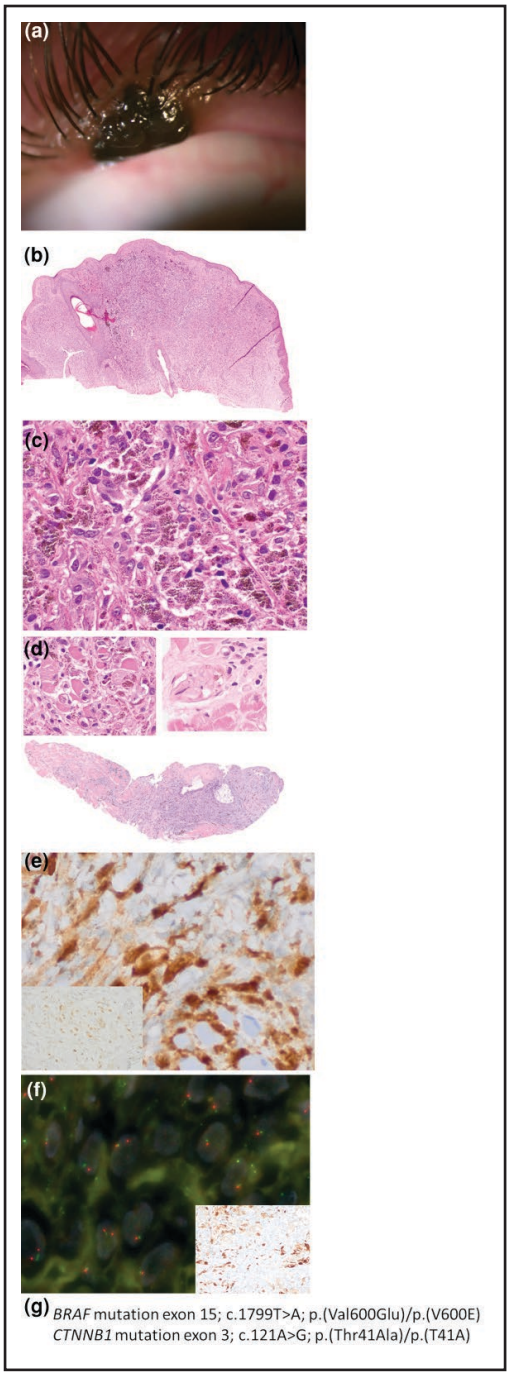

Figure 1 Combined WNT-activated deep-penetrating/plexiform melanocytoma (DPM) in the eyelid conjunctiva (patient 4). (a) Clinical picture showing an asymmetrical, irregular and darkly pigmented nodule that grew rapidly. (b) Histopathological image showing two distinctive areas: common naevus on the left and DPM on the right. Haematoxylin and eosin (H&E), panoramic × 2. (c) The DPM component was composed of large epithelioid cells with high-grade nuclear atypia and finely pigmented cytoplasm. Nuclei were vesiculous, hyperchromatic, with a large visible nucleolus. H&E, × 60. (d) Deep portion of the resection showing absence of in-depth maturation and infiltration of the muscle (left inset) and neurotropism (right inset). H&E, panoramic × 2, left and right insets × 60. (e) Nuclear positivity for β-catenin and LEF1 (inset) in the DPM component [immunohistochemistry (IHC), × 60]. (f) 9p21 fluorescence *in situ* hybridization (FISH) probe showed *CDKN2A* heterozygous loss: most of the cells harbour only one red signal (*CDKN2A*). The tumour cells showed p16 loss (9p21, FISH; insight, p16). IHC × 40. (g) The lesion harboured both *BRAF*V600E and exon 3 *CTNNB1* mutations (next-generation sequencing).

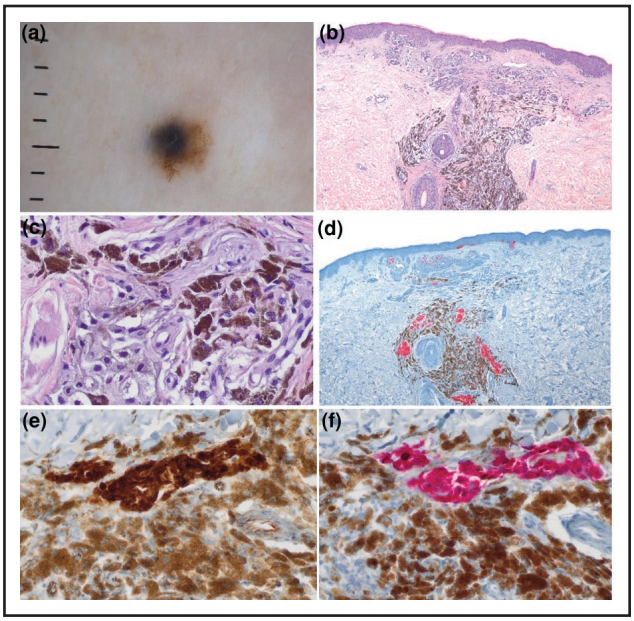

Figure 2 Combined WNT-activated deep-penetrating/plexiform melanocytoma (DPM) in the trunk (patient 45). (a) Clinical picture showing a small lesion of 3 mm, with rapid and asymmetrical growth from a pre-existing naevus. Dermoscopy showed a blue structureless area over a common naevus pattern. (b) Histopathological image showing two distinctive areas: common naevus on the left and DPM on the right, showing a deep, asymmetrical and plexiform growth. Mild fibrosis and abundant melanophages predominated in the DPM component. Haematoxylin and eosin (H&E), panoramic × 2. (c) The DPM component showed epithelioid and some spindle melanocytes with moderate atypia, pleomorphism and finely pigmented cytoplasm. H&E, × 60. (d) DPM component cells retaining positivity for HMB45; notice the abundant melanophages. Immunohistochemistry (IHC), × 2. (e) Nuclear positivity for β-catenin in the DPM component. IHC, × 60. (f) Double stain (Melan-A + Ki67) showing proliferation in less than 2% of the melanocytes. IHC, × 60.

Junctional activity was seen in 12 patients (24%), but pagetoid spread was not seen in any patients. In nine patients (18%), the DPM component showed an extensive, deep, asymmetrical and plexiform pattern, whereas in two the DPM components (4%) showed nodular, expansile growth (Figure 3). The DPM component was composed of large, epithelioid, sometimes elongated cells, exhibiting finely pigmented cytoplasm. Nuclei were vesiculous with visible nucleoli. Absence of in-depth maturation was a common feature. Moderate atypia with nuclear pleomorphism was seen in most; only two (4%) exhibited high-grade atypia. Mitotic figures were infrequent (12%), and always < 2 per mm^2. Atypical histological features in the DPM component (≥ 5 mm, asymmetry, with expansile growth and high-grade atypia) were seen in 10 patients (20%) (Figure 1 and Figure 3).

The tumour microenvironment showed frequent vascular hyperplasia, a mild inflammatory lymphoid component, mild fibrosis, as well as the presence of melanophages. Melanophages were abundant, focally showing large groups in five patients (10%) (Figure 2).

Nuclear immunohistochemistry (IHC) positivity for β-catenin and LEF1 was seen in the DPM component of all patients (Figures 1–3). In 45 patients (88%), common naevi cells, especially those located below the epidermis or beside the follicle structures, also showed β-catenin and LEF1 nuclear positivity (Figure 3).

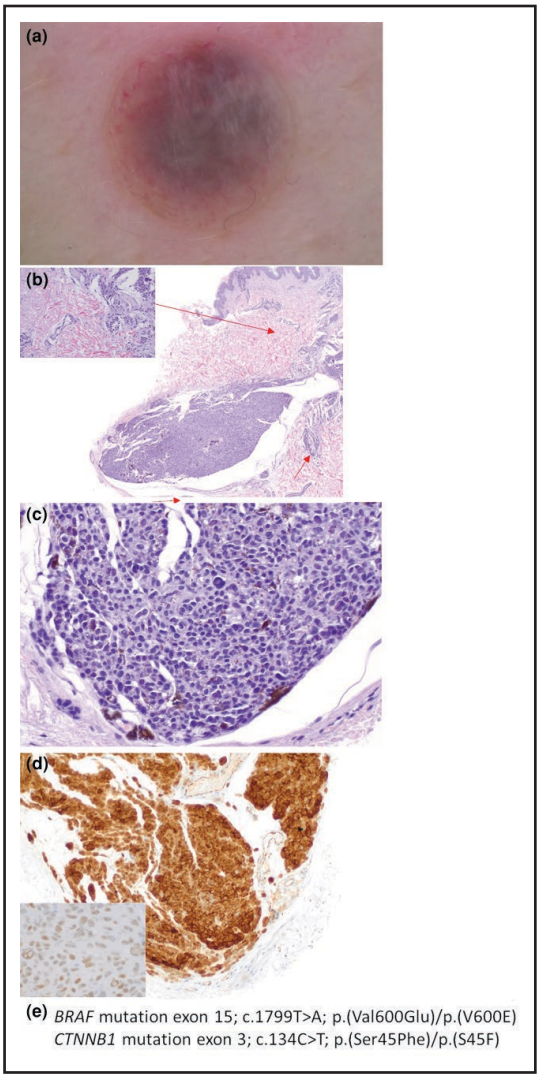

Figure 3 Combined WNT-activated deep-penetrating/plexiform melanocytoma (DPM) in the lumbar region (patient 41). (a) Dermoscopic image showing polychromatism with blue–grey areas and prominent vascularization (comma vessels). (b) Histopathological image showing two distinctive areas: common naevus in the superior part of the lesion and DPM showing deep nodular expansile growth. Notice the prominent vascularization around and inside the lesion (red arrows and inset). Haematoxylin and eosin (H&E), panoramic × 2, inset × 60. (c) DPM component was composed of epithelioid melanocytes with moderate atypia and pleomorphism. H&E, × 40. (d) Nuclear positivity for β-catenin and LEF1 (inset) in the DPM component. Immunohistochemistry, × 40, inset × 60. (e) The lesion harboured both *BRAF*^{V600E} and exon 3 *CTNNB1* mutations (next-generation sequencing).

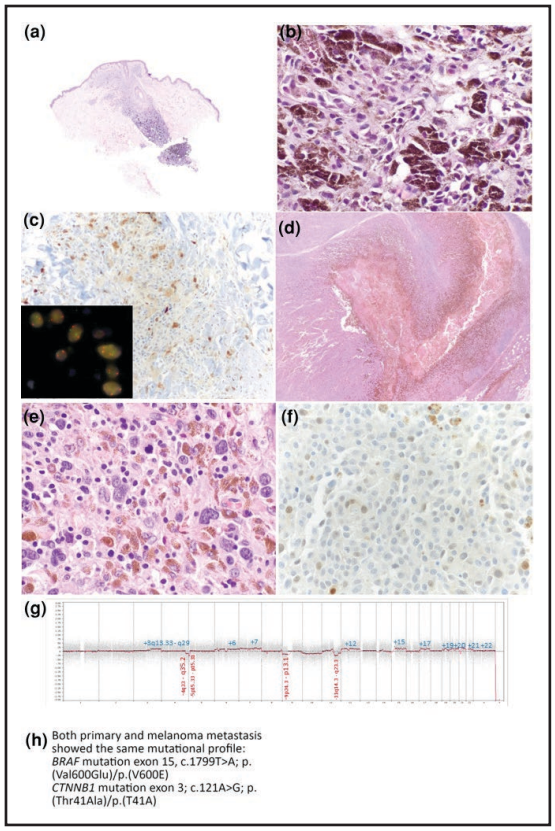

Figure 4 Combined WNT-activated deep-penetrating/plexiform melanocytoma (DPM) in the left leg, incompletely excised (a–c) and melanoma metastasis in the ipsilateral inguinal lymph node that appeared 10 years later (d–f) (patient 49). (a) Histopathological image showing two distinctive areas: common naevus in the superior area of the lesion and DPM component showing wedge-shaped and plexiform growth around a follicle structure. Haematoxylin and eosin (H&E), panoramic × 2. (b) At a higher magnification, melanocytes showed moderate pleomorphism, and abundant melanophages were observed. H&E, × 60. (c) The tumour cells showed p16 loss [immunohistochemistry (IHC), × 40], but without abnormalities in the 9p21 locus assessed by fluorescence *in situ* hybridization (FISH): two red signals (*CDKN2A*) are counted in all tumoral cells (inset, FISH). (d) The melanoma metastasis in an inguinal lymph node showed abundant melanophages and necrosis. H&E, panoramic × 2. (e) At a higher magnification, high-grade atypical cells with pleomorphic nuclei and a large visible nucleoli were seen. H&E, × 60. (f) Complete p16 loss. IHC, × 40. (g) Copy-number (CN) array showed multiple losses affecting regions 4q33-q35.2, 5p15.33-p15.31, 9p24.4-p13.11 and 11q14.3-q23.3; gains were seen in regions 3q13.33-q29, 6p25.3-q13, 6q15-q27, 7p22.3-q36.3, 12p13.33-q24.33, 15q11.1-q26.3, 17p13.3-q25.3, 19p13.3-q13.43, 20p13-q13.33, 21p11.2-q22.3 and 22q11.1-q13.33. Notice the loss of 9p24.3-p13.1 where the *CDKN2A* gene is located (CN array). (h) Both the primary combined DPM and melanoma metastasis showed the same mutational profile: *BRAF*^{V600E} and exon 3 *CTNNB1* mutations (next-generation sequencing).

A loss of p16 was seen in the DPM component of seven patients (14%); four of these showed atypical histological features (Figure 1). A high Ki67 score (over 5%) was seen in two (4%), both showing atypical histological features (size ≥ 5 mm, poor circumscription, asymmetry and high-grade atypia).

Molecular studies

Samples from 13 patients (25%), including those with atypical histological features and/or aberrant immunohistochemical results, were submitted for further molecular studies, including NGS, detection of *TERT*p mutations by Sanger sequencing and 9p21 locus exploration by FISH.

The multiprobe FISH for melanoma and CN array were performed in the primary combined DPM that developed melanoma metastasis and were applied from both tumoral samples (primary tumour and metastasis).

Next-generation sequencing and TERT-promoter mutation results

The NGS panel gave valid results in 11 of the 13 samples from patients explored. All 11 harboured both *BRAF*^{V600E} and exon 3 *CTNNB1* mutations. Two different exon 3 *CTNNB1*

mutations were detected: c.121A>G; p.(Thr41Ala)/p.(T41A) in seven patients and c.134C>T; p.(Ser45Phe)/p.(S45F) in four patients.

In two patients, only *BRAF*^{V600E} was detected despite the strong positivity for β-catenin and LEF1 of the DPM component because of the large number of melanophages and the scarcity of tumoral cells analysed (Figure 2). *TERT*p mutations were detected in none, even in the melanoma metastasis specimen.

9p21 analysis

Only one combined DPM arising in the conjunctiva, showing atypical histological features and p16 loss, harboured *CDKN2A* heterozygous loss by FISH (Figure 1). The rest of the combined DPMs did not show *CDKN2A* abnormalities by FISH (Table 1).

The melanoma metastasis did not show valid 9p21 FISH results as an increased CN of several genes was seen, according to aneuploidy. Nevertheless, the CN array performed in this sample showed a loss of 9p24.3-p13.1 where the *CDKN2A* gene is located (Figure 4).

Fluorescence in situ hybridization melanoma multiprobe and copy-number array results

The combined DPM that developed melanoma metastasis did not meet the FISH criteria for melanoma. The melanoma metastasis showed an increased CN of *RREB1*, *CNND1* and centromere of chromosome 6 according to aneuploidy. Paired CN analysis of the primary combined DPM and melanoma metastasis was performed by Oncoscan array in this sample. Nevertheless, the CN profile was not valid in the primary combined DPM because of the low quality of the DNA extracted. Conversely, in the melanoma metastasis, in addition to aneuploidy, CN array showed multiple losses affecting regions 4q33-q35.2, 5p15.33-p15.31, 9p24.4-p13.11 and 11q14.3-q23.3; gains were seen in regions 3q13.33-q29, 6p25.3-q13, 6q15-q27, 7p22.3-q36.3, 12p13.33-q24.33, 15q11.1-q26.3, 17p13.3-q25.3, 19p13.3-q13.43, 20p13-q13.33, 21p11.2-q22.3 and 22q11.1-q13.33. Notice the loss of 9p24.3-p13.1, where the *CDKN2A* gene is located (Figure 4).

Discussion

Since the well-defined histopathological and molecular characterization of DPM has been updated,[3,4,14] this is the first report, to the best of our knowledge, to include a series of combined DPMs. In all patients, an acquired clone had developed a WNT-activated melanocytic tumour or melanocytoma from a common acquired or congenital-type naevus.

In our series, in 68% of patients, the acquired and progressive growth, as well as changes in pigmentation, have frequently hampered the differentiation from malignant melanoma, in agreement with previous reports on combined naevi.[1] Dermoscopically the blue structureless areas frequently seen in combined blue naevi[18–20] were seen in all but one of our patients, thus suggesting the possibility of a differential diagnosis with the grey–blue veil of melanomas. In addition, our patients' samples frequently showed signs of prominent vascularization, such as erythema, comma vessels and polychromatism, which agree with the marked vascularization histologically observed in most of our patients' cases. Although polychromatism can be seen in melanomas, it has also been described in DPMs[21,22]; however, white lines, thick reticular lines and a chaotic architecture that are dermoscopically highly suspicious of melanoma diagnosis are rarely seen in combined naevi.[23] Our findings corroborate a clinical and dermoscopic overlapping of combined naevi with that of melanoma in some cases. Therefore, they support the recommendation of complete excision of combined DPM, even in low-grade tumours, with at least a 2 mm margin, as it is considered an intermediate melanocytic tumour or melanocytoma.[23]

Histologically, the diagnosis of combined DPM must be suspected when a wedge-shaped and plexiform, deep melanocytic component, composed of large epithelioid or spindle-shaped cells, grows inside a common or congenital-type naevus. However, the DPM component can show diverse architectural and cytological morphologies, such as a superficial growth above the common naevus component, and junctional activity, which we have seen in 10% and 24% of our patients, respectively.

IHC for β-catenin and LEF-1, markers of WNT pathway activation, can confirm the diagnosis by demonstrating nuclear positivity.[4,24,25] In most of the combined DPMs in our series, there was nuclear expression of these markers also in a subset of naevomelanocytic cells located beside the epithelial structures (below the epidermis and beside the follicular structures) of the common or congenital-type naevus. The increased β-catenin signalling in these cells, although lacking *CTNNB1* mutations, gives the potential for naevus cells to grow and transform, according to previous reports.[4,26] These naevomelanocytic cells already harbour a MAPK-activated oncogene mutation, usually *BRAF*^{V600E},[27] and can acquire an additional WNT-activating mutation that develops into a combined DPM.[28]

The NGS panel that we used in this study covers the main mutation gene drivers of nonatypical and atypical DPMs.[4,14,27] In all samples with valid results, we found a mutation involving both *BRAF*^{V600E} and exon 3 *CTNNB1*. Other mutations involving genes that activate the MAPK and WNT pathways, including *HRAS*, *NRAS*, *MAPK2K1* and *APC*, have been described in DPMs.[4,27] Although *IDH1* mutations have also been described in atypical DPMs,[27] none were identified in our patients. Nevertheless, the double mutation of *BRAF*^{V600E} and exon 3 *CTNNB1* is the most frequent profile that has been documented in combined DPMs, in agreement with our results.[4,27,28]

Challenging atypical histopathological features regarding the DPM component, including the large size of the lesion, asymmetry, expansile growth and high-grade atypia were seen in 20% of patients in our series. From a histopathological point of view, these atypical features can pose a challenging differential diagnosis with melanoma developing from a naevus. Atypical architectural and cytological features have been previously reported in combined naevi, in about 47% of combined Spitz tumours and 26% of combined DPMs in a large series.[2] It is important to be aware of these cytoarchitectural variations in order to avoid the misdiagnosis of melanoma arising in a pre-existing naevus.

Owing to the diagnostic and prognostic significance of p16 loss, Ki67 proliferative index and PRAME expression

in DPMs,[14] these immunostains have been explored in all our samples. A loss of p16 expression was observed in seven (14%). This p16 immunostain pattern compelled us to explore the *CDKN2A* gene status in order to ascertain its biological significance. In all samples, *CDKN2A* mutations were ruled out by NGS analysis. 9p21 exploration by FISH showed only one patient harbouring *CDKN2A* heterozygous loss and none with *CDKN2A* homozygous loss. These results are in line with previously reported DPMs and Spitz melanocytomas,[14,16] in which partial but significant p16 loss, without *CDKN2A* gene abnormalities or heterozygous *CDKN2A* loss, do not have prognostic significance.

In our series, all but one patient had a favourable follow-up, concurring with the low risk of malignant transformation of combined DPMs observed in previously published studies.[3,14] Only one combined DPM, partially removed, presented a regional lymph node melanoma metastasis 10 years later. The primary tumour lacked significant cytoarchitectural atypia, mitoses and *CDKN2A* anomalies by FISH, despite partial loss of p16 immunostain. The Ki67 proliferative index was $<5\%$, PRAME was negative and multiprobe melanoma FISH showed no abnormalities. Conversely, the metastatic melanoma exhibited CN variations, including loss of 9p21-24 (*CDKN2A* location), detected by CN array. No *TERT*p mutations were found and both tumours showed the *BRAF*^{V600E} and exon 3 *CTNNB* double mutation. Previous reports on DPMs developing into malignant melanomas[12–14] have stressed the absence of molecular alterations before the malignant development, in agreement with our results. Conversely, the melanomas developed from DPMs often involve *CDKN2A* deletion, as seen in our patient, and additional molecular alterations, such as *TERT*p mutation have been reported.[4,14]

The study's strengths lie in it being a large series with complete histopathology and with follow-up data, showing that almost all the studied patients had a favourable outcome, despite 20% of them having histological atypical features. This apparent discordance between morphology and prognosis requires further investigation; however, various factors might be involved in preventing progression towards malignancy including immune response, microenvironment and perhaps melanocytoma may have more genetic stability and may lack the full range of genetic alterations frequently involved in melanomas. The study has limitations that include incomplete clinical data and incomplete molecular profiling in some patients' cases because of insufficient DNA quality.

In conclusion, we present a series of patients with combined DPMs that warrant complete excision because of the potential for atypical features and malignant transformation.

Acknowledgements

The authors thank Itziar Salaverria for performing the copy-number array analysis (Oncoscan).

Funding sources

This research received no specific grant from any funding agency in the public, commercial or not-for-profit sectors.

Conflicts of interest

The authors declare no conflicts of interest.

Data availability

The data underlying this article will be shared upon reasonable request to the corresponding author.

Ethics statement

Ethical approval: This study was conducted in accordance with the principles of the Declaration of Helsinki (as revised in 2013) and was approved by the Internal Review Board of the Hospital Clinic of Barcelona (HCB/2017/0097). All patient data were anonymous. Informed consent: All patients gave written, informed consent for participation and publication of their case details and images.

References

1 Scolyer RA, Zhuang L, Palmer AA *et al.* Combined naevus: a benign lesion frequently misdiagnosed both clinically and pathologically as melanoma. *Pathology* 2004; **36**:419–27.
2 Baran JL, Duncan LM. Combined melanocytic nevi. *Am J Surg Pathol* 2011; **35**:1540–8.
3 Lazar A, Scoyler R, de la Fouchardière A *et al.* Melanocytic tumours. In: *WHO Classification of Tumours Editorial Board. Skin Tumours* (Elder D, Barnhill R, eds), 5th edn, vol. **12**. Lyon: International Agency for Research on Cancer, 2023.
4 Yeh I, Lang UE, Durieux E *et al.* Combined activation of MAP kinase pathway and β-catenin signaling cause deep penetrating nevi. *Nat Commun* 2017; **8**:644.
5 Garrido MC, Nájera L, Navarro A *et al.* Combination of congenital and deep penetrating nevus by acquisition of β-catenin activation. *Am J Dermatopathol* 2020; **42**:948–52.
6 Hung T, Yang A, Mihm MC, Barnhill RL. The plexiform spindle cell nevus nevi and atypical variants: report of 128 cases. *Hum Pathol* 2014; **45**:2369–78.
7 High WA, Alanen KW, Golitz LE. Is melanocytic nevus with focal atypical epithelioid components (clonal nevus) a superficial variant of deep penetrating nevus? *J Am Acad Dermatol* 2006; **55**:460–6.
8 Barnhill RL. Melanocytic nevi with phenotypic heterogeneity. In: *Pathology of Melanocytic Nevi and Malignant Melanoma* (Barnhill RL, Piepkorn MW, Basuam KJ eds). New York: Springer, 2014, 301–29.
9 Dadras SS, Lu J, Zembowicz A *et al.* Histological features and outcome of inverted type-A melanocytic nevi. *J Cutan Pathol* 2018; **45**:254–62.
10 Seab JA, Graham JH, Helwig EB. Deep penetrating nevus. *Am J Surg Pathol* 1989; **13**:39–44.
11 Robson A, Morley-Quante M, Hempel H *et al.* Deep penetrating naevus: clinicopathological study of 31 cases with further delineation of histological features allowing distinction from other pigmented benign melanocytic lesions and melanoma. *Histopathology* 2003; **43**:529–37.
12 Magro CM, Abraham RM, Guo R *et al.* Deep penetrating nevus-like borderline tumors: a unique subset of ambiguous melanocytic tumors with malignant potential and normal cytogenetics. *Eur J Dermatol* 2014; **24**:594–602.
13 Isales MC, Khan AU, Zhang B *et al.* Molecular analysis of atypical deep penetrating nevus progressing to melanoma. *J Cutan Pathol* 2020; **47**:1150–4.

14 Ebbelaar CF, Schrader AMR, van Dijk M *et al*. Towards diagnostic criteria for malignant deep penetrating melanocytic tumors using single nucleotide polymorphism array and next-generation sequencing. *Mod Pathol* 2022; **35**:1110–20.
15 Cosgarea I, Griewank KG, Ungureanu L *et al*. Deep penetrating nevus and borderline-deep penetrating nevus: a literature review. *Front Oncol* 2020; **10**; https://doi.org/10.3389/fonc.2020.00837
16 Harms PW, Hocker TL, Zhao L *et al*. Loss of p16 expression and copy number changes of CDKN2A in a spectrum of spitzoid melanocytic lesions. *Hum Pathol* 2016; **58**:152–60.
17 Díaz A, Valera A, Carrera C *et al*. Pigmented spindle cell nevus: clues for differentiating it from spindle cell malignant melanoma. A comprehensive survey including clinicopathologic, immunohistochemical, and FISH studies. *Am J Surg Pathol* 2011; **35**:1733–42.
18 Schweizer A, Fink C, Bertlich I *et al*. Differentiation of combined nevi and melanomas: case-control study with comparative analysis of dermoscopic features. *J Dtsch Dermatol Ges* 2020; **18**:111–18.
19 De Giorgi V, Massi D, Salvini C *et al*. Dermoscopic features of combined melanocytic nevi. *J Cutan Pathol* 2004; **31**:600–4.
20 Stojkovic-Filipovic J, Tiodorovic D, Lallas A *et al*. Dermatoscopy of combined blue nevi: a multicentre study of the International Dermoscopy Society. *J Eur Acad Dermatol Venereol* 2021; **35**:900–5.
21 Strazzula L, Senna MM, Yasuda M, Belazarian L. The deep penetrating nevus. *J Am Acad Dermatol* 2014; **71**:1234–40.
22 Robles-Tenorio A, Preciado-Aguiar MS, Quiñones-Venegas R, Salazar-Torres FJ. Dermoscopic rainbow pattern in a deep penetrating nevus. *Dermatol Pract Concept* 2022; **12**:e2022046.
23 de la Fouchardiere A, Blokx W, van Kempen LC *et al*. ESP, EORTC, and EURACAN expert opinion: practical recommendations for the pathological diagnosis and clinical management of intermediate melanocytic tumors and rare related melanoma variants. *Virchows Arch* 2021; **479**:3–11.
24 de la Fouchardière A, Caillot C, Jacquemus J *et al*. β-Catenin nuclear expression discriminates deep penetrating nevi from other cutaneous melanocytic tumors. *Virchows Arch* 2019; **474**:539–50.
25 Raghavan SS, Saleem A, Wang JY *et al*. Diagnostic utility of LEF1 immunohistochemistry in differentiating deep penetrating nevi from histologic mimics. *Am J Surg Pathol* 2020; **44**:1413–18.
26 Pawlikowski JS, McBryan T, van Tuyn J *et al*. Wnt signaling potentiates nevogenesis. *Proc Natl Acad Sci U S A* 2013; **110**:16009–14.
27 Manca A, Sini MC, Cesinaro AM *et al*. NGS-based analysis of atypical deep penetrating nevi. *Cancers (Basel)* 2021; **13**:3006.
28 Šekoranja D, Vergot K, Hawlina G, Pižem J. Combined deep penetrating nevi of the conjunctiva are relatively common lesions characterised by BRAFV600E mutation and activation of the beta catenin pathway: a clinicopathological analysis of 34 lesions. *Br J Ophthalmol* 2020; **104**:1016–21.